Electronic Supplementary Material (ESI) for Nanoscale.

Supporting Information

Synthesis of morphology-tunable electroactive biomass/graphene composites by metal ions for supercapacitors

Changlun Xiong,[a] Yubo Zou,[a] Zhiyuan Peng, Wenbin Zhong*

College of Materials Science and Engineering, Hunan University, Changsha, China.

[a] These authors contributed equally to this work.

* Corresponding author, Email: wbzhong@hnu.edu.cn

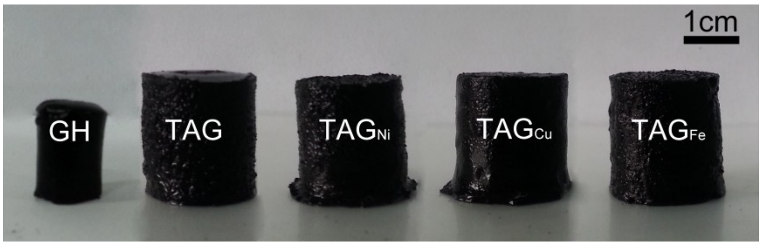

Fig. S1 Photograph of the as-prepared GH, TAG, TAG_{Ni}, TAG_{Cu} and TAG_{Fe} by hydrothermal assembled processes.

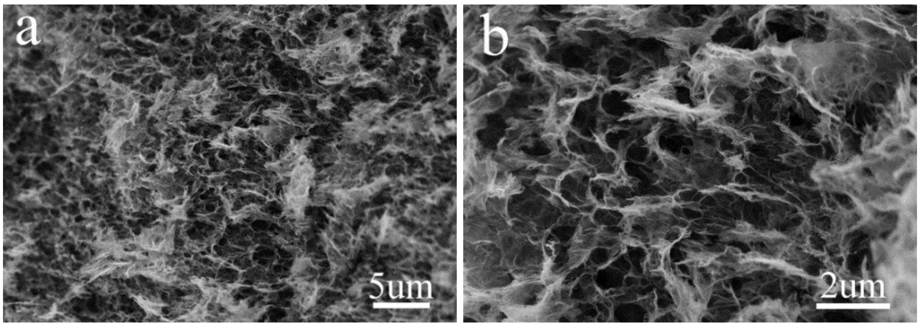

Fig. S2 SEM images of GH.

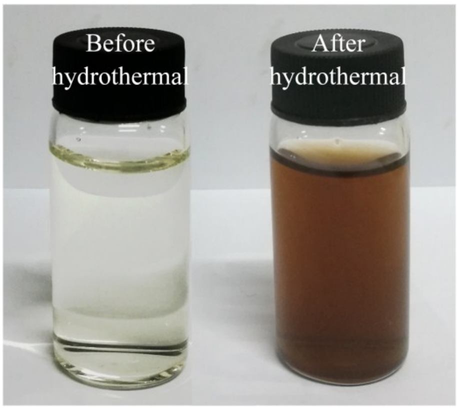

Fig. S3 The photographs of TA before (left) and after (right) hydrothermal process.

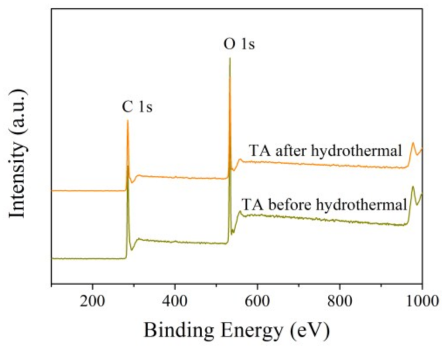

Fig. S4 The XPS spectra of TA before and after hydrothermal process.

Table S1 Parameters of porous structures calculated from nitrogen adsorption/desorption isotherms (SSA: Specific Surface Area).

Sample	SSA_{total} (m^2 g^{-1})	$SSA_{mesopores}$ (m^2 g^{-1})	$SSA_{micropores}$ (m^2 g^{-1})	Pore volume (cm^3 g^{-1})
GH	152	135.8	16.2	0.50
TAG	127	127	0	0.52
TAG_{Ni}	159	159	0	0.49
TAG_{Cu}	125	114	11	0.24
TAG_{Fe}	127	127	0	0.57

Table S2 The element contents of GO, TA, TA after hydrothermal, GH, TAG, TAG_{Ni}, TAG_{Cu} and TAG_{Fe}.

Samples	GO	TA	TA after hydrothermal	GH	TAG	TAG_{Ni}	TAG_{Cu}	TAG_{Fe}
C (at.%)	66.01	63.29	67.72	86.66	78.84	80.89	84.38	80.86
O (at.%)	33.99	36.71	32.28	13.34	21.16	19.11	15.62	19.14

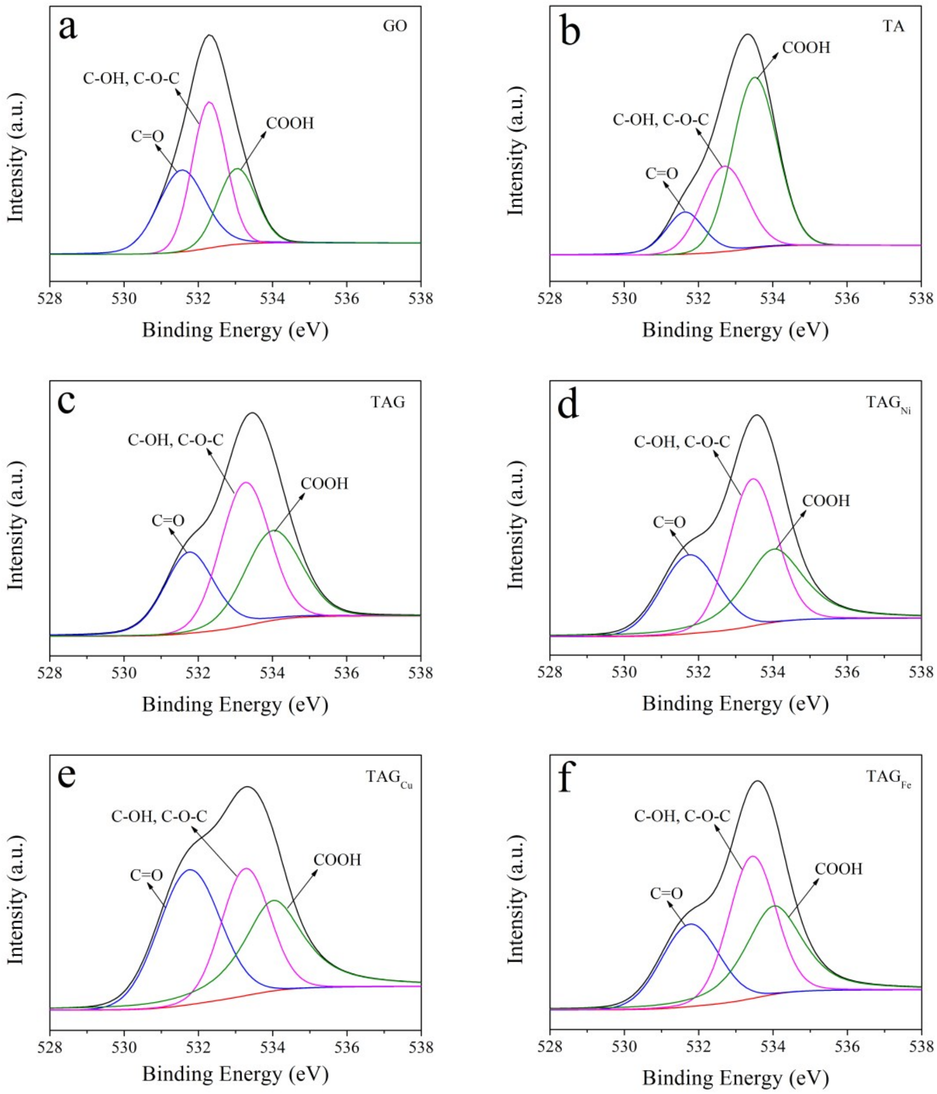

Fig. S5 The O 1s spectra of (a) GO, (b) TA, (c) TAG, (d) TAG$_{Ni}$, (e) TAG$_{Cu}$ and (f) TAG$_{Fe}$.

The O 1s spectrum of GO, TA, TAG, TAG$_{Ni}$, TAG$_{Cu}$ and TAG$_{Fe}$ can be curve-fitted into three peaks: C=O (~531.6 eV), C-OH, C-O-C (~532.7 eV) and COOH (~534 eV).

Table S3 Relative ratio (at.%) of different oxygen components in GO, TA, TAG,TAG_{Ni}, TAG_{Cu} and TAG_{Fe} from O 1s XPS spectra.

Samples	C=O	C-OH, C-O-C	COOH
GO	34.2	41.6	24.2
TA	13.4	29.2	57.4
TAG	26.7	42.0	31.3
TAG_{Ni}	25.6	41.9	32.5
TAG_{Cu}	37.4	28.6	34.0
TAG_{Fe}	26.1	38.4	35.5

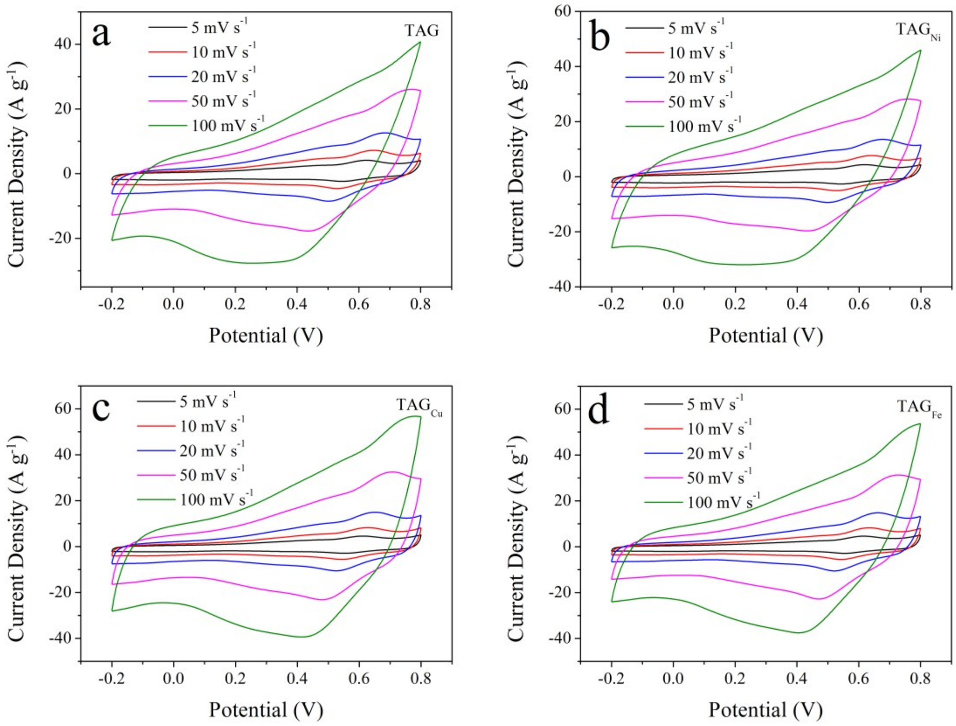

Fig. S6 CV curves of (a) TAG, (b) TAG_{Ni}, (c) TAG_{Cu} and (d) TAG_{Fe} at various scan rates.

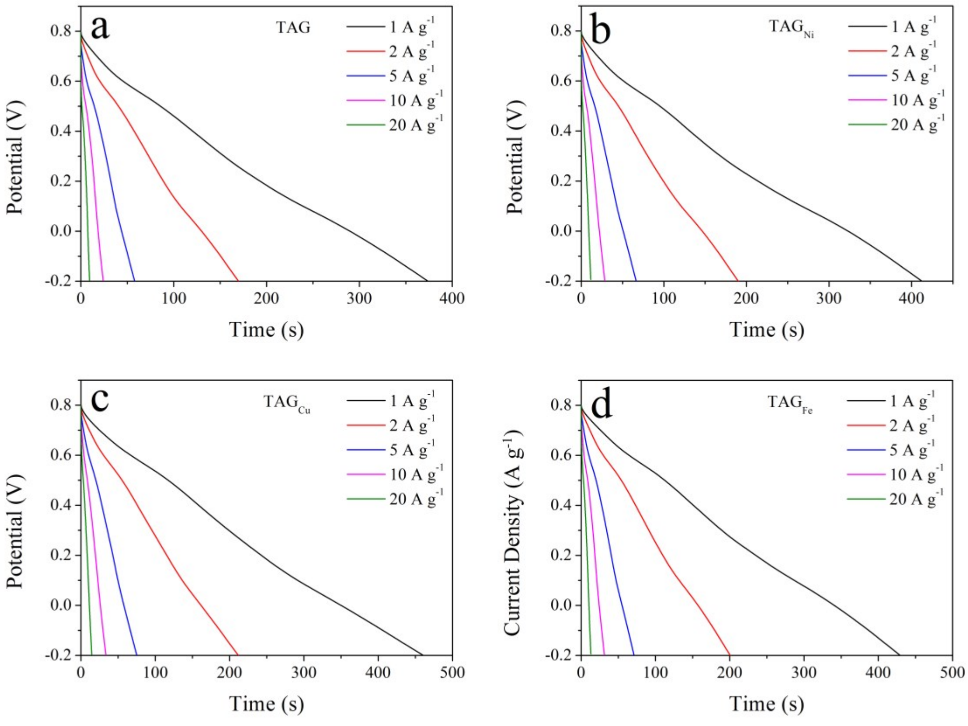

Fig. S7 Discharge curves of (a) TAG, (b) TAG_{Ni}, (c) TAG_{Cu} and (d) TAG_{Fe} at different current densities.

Table S4 Comparison of specific capacitance of TAG_{Ni}, TAG_{Cu} and TAG_{Fe} with reported conducting polymer hydrogels, conducting polymer/garphene hydrogels or aerogels, biomass based composites and graphene/carbon materials based on a three-electrode system and two-electrode system.

Materials	Current density / Scan rate	C_s (F g^{-1})	Reference
conductive polypyrrole hydrogels	0.2 A g^{-1}	380	[S1]
conducting polyaniline hydrogels	5 mV s^{-1}	430	[S2]
graphene/PANI hybrid aerogel	0.25-2 A g^{-1}	520.3-333	[S3]
rGO/polyaniline nanofiber hybrids	1 A g^{-1}	475	[S4]
3D graphene/polyaniline hydrogel	2 A g^{-1}	334	[S5]

polypyrrole-mediated graphene foam	1.5 A g^{-1}	350	[S6]
graphene/polypyrrole aerogels	0.5 A g^{-1}	304	[S7]
rGO/polypyrrole hydrogels	1 A g^{-1}	473	[S8]
cellulose nanofiber/RGO aerogel	5 mV s^{-1}	207	[S9]
CNF/RGO/CNT aerogels	0.5 A g^{-1}	252	[S10]
polyaniline/lignosulfonate composites	10 A g^{-1}	377.2	[S11]
rGO/lignosulfonate composites	10 mV s^{-1}	432	[S12]
PPy/LGS-coated fabric	0.1 A g^{-1}	304	[S13]
graphene/N-doped carbon	0.2 A g^{-1}	377	[S14]
Graphene/N-doped carbon	1 A g^{-1}	290.2	[S15]
activated carbon xerogels	2 mV s^{-1}	239	[S16]
TAG_{Ni}	**1-20 A g^{-1}**	**412.4-228**	**This work**
TAG_{Cu}	**1-20 A g^{-1}**	**460.4-286**	**This work**
TAG_{Fe}	**1-20 A g^{-1}**	**429.4-258**	**This work**

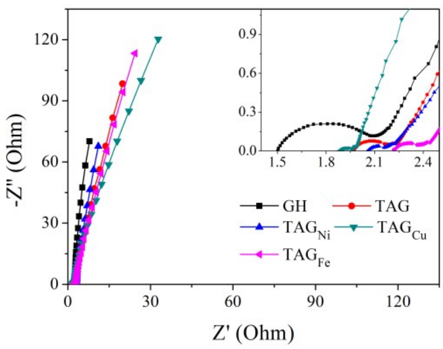

Fig. S8 Nyquist plots of GH, TAG, TAG$_{Ni}$, TAG$_{Cu}$ and TAG$_{Fe}$ (the inset shows the magnified high-frequency regions).

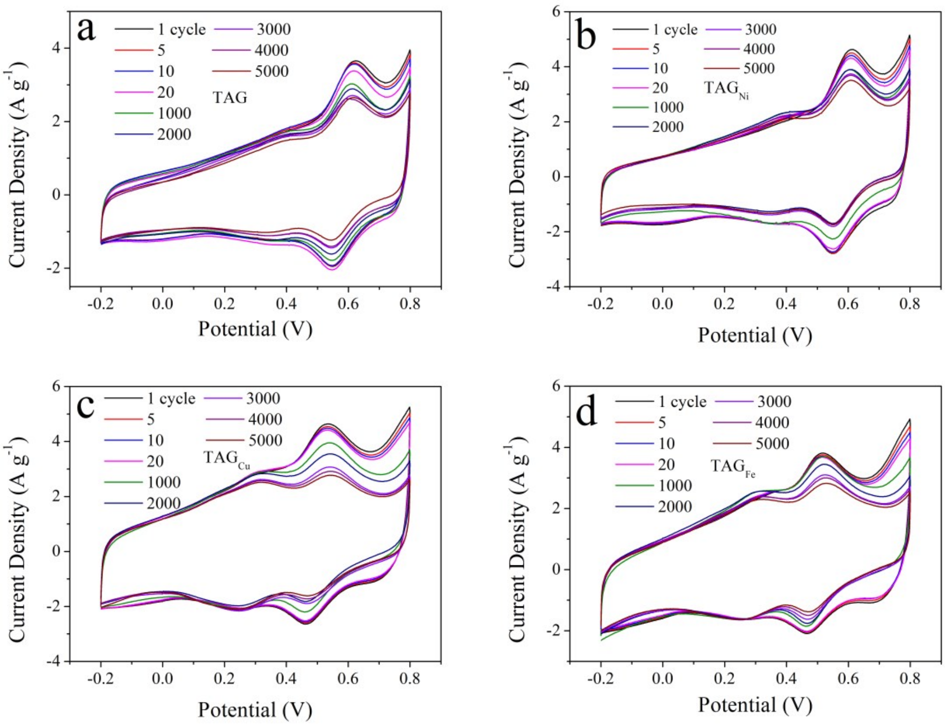

Fig. S9 The CV curves of TAG, TAG$_{Ni}$, TAG$_{Cu}$ and TAG$_{Fe}$ electrodes at 5 mV s^{-1} after different cycles.

Table S5 The cycling stability of TAG_{Ni}, TAG_{Cu} and TAG_{Fe} compared to reported conducting polymer/graphene hydrogels, biomass based composites and carbon materials based on a three-electrode system.

Materials	Current density / Scan rate	Cycling stability	Reference
rGO/polyaniline hybrids	1 A g^{-1}	1000 (86%)	[S4]
3D graphene/polyaniline hydrogel	2 A g^{-1}	1000 (77%)	[S5]
PANI/rGO hydrogel	8 A g^{-1}	1000 (77%)	[S17]
Polypyrrole/graphene hydrogels	5 A g^{-1}	4000 (87%)	[S18]
rGO/polypyrrole hydrogels	5 A g^{-1}	1000 (82%)	[S8]
graphene/polypyrrole hydrogels	10 A g^{-1}	1000 (80%)	[S19]
3D rGO/cellulose composites	0.15 A g^{-1}	100 (90%)	[S20]
CNFs/MWCNTs/PANI	2 A g^{-1}	1000 (82.4%)	[S21]
polyaniline/lignosulfonate composites	1 A g^{-1}	1000 (74.3%)	[S11]
PPy/LGS-coated fabric	0.2 A g^{-1}	300 (76%)	[S13]
PPY/HMA/lignin composites	1 A g^{-1}	1000 (74%)	[S22]
PEDOT/Lignin biopolymer composites	8 A g^{-1}	1000 (83%)	[S23]
N-doped porous carbon/graphene	2 A g^{-1}	2000 (90%)	[S24]
RCG	50 mV s^{-1}	2000 (93.3%)	[S25]
activated carbons	1 A g^{-1}	1000 (90%)	[S26]
TAG_{Ni}	**20 A g^{-1}**	**1000 (92.1%)** **5000 (78.0%)**	**This work**
TAG_{Cu}	**20 A g^{-1}**	**1000 (90.5%)**	**This work**

		5000 (76.0%)	
TAG_{Fe}	20 A g^{-1}	1000 (93.5%) 5000 (79.9%)	This work

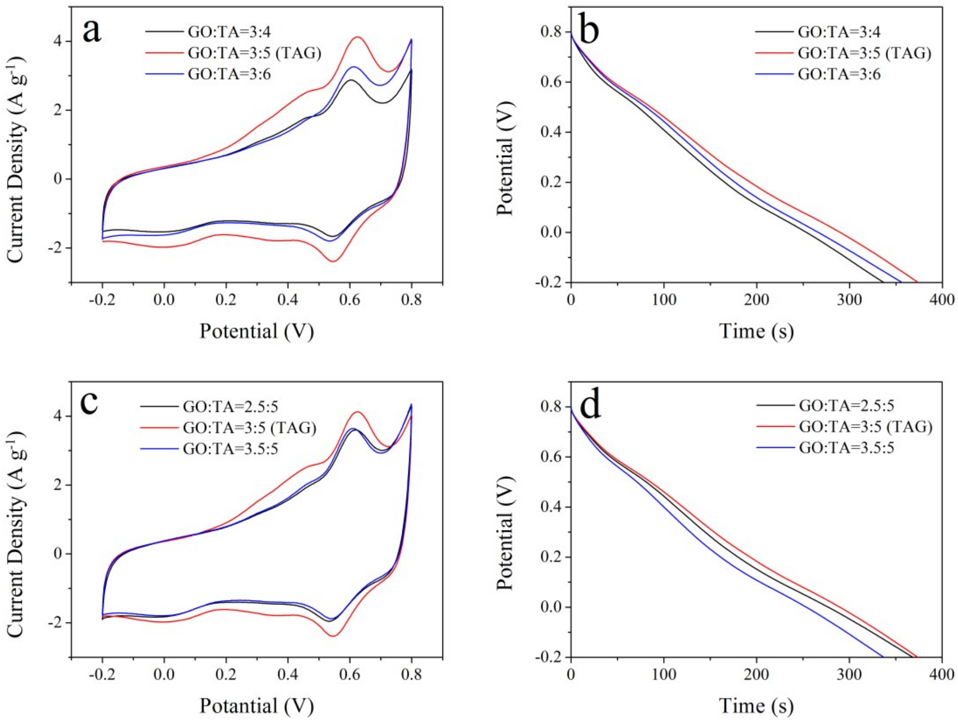

Fig. S10 The electrochemical properties of TAG at different mass ratio (a, b) R_m (GO:TA) = 3:4, 3:5 and 3:6, (c, d) R_m (GO:TA) = 2.5:5, 3:5 and 3.5:5, ((a, c) CV curves at 5 mV s^{-1} and (b, d) discharge curves at 1 A g^{-1}).

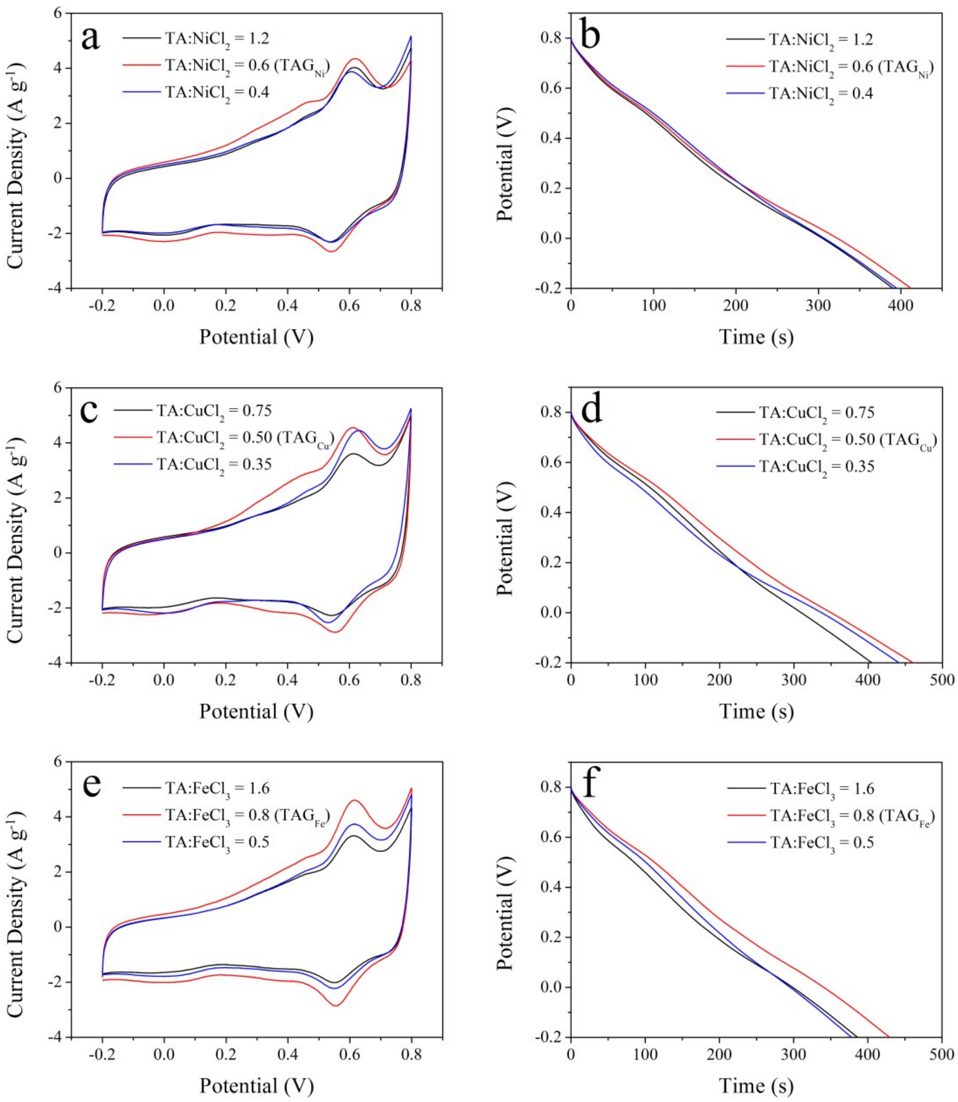

Fig. S11 The electrochemical properties of TA/graphene composites based on R_m (GO:TA) = 3:5 and different molar ratio of TA to metal chlorides ($NiCl_2$, $CuCl_2$ and $FeCl_3$): (a, b) n(TA) : n($NiCl_2$) = 1.2, 0.6 and 0.4, (c, d) n(TA) : n($CuCl_2$) = 0.75, 0.50 and 0.35, (e, f) n(TA) : n($FeCl_3$) = 1.6, 0.8 and 0.5. (a, c, e) CV curves at 5 mV s^{-1} and (b, d, f) discharge curves at 1 A g^{-1}.

Table S6 Comparison of specific capacitance of TAG_{Ni}, TAG_{Cu} and TAG_{Fe} with reported conducting polymer/garphene composites and biomass based composites based on a two-electrode system.

Materials	Current density / Scan rate	C_s (F g^{-1})	Reference
IPCN850@dopa@Fe-TA	5 mV s^{-1}	~244	[S27]
RL-60	1 A g^{-1}	203	[S12]
AQDS-GPy	1 A g^{-1}	237	[S28]
PPy-RGO composites	0.2 A g^{-1}	255.7	[S29]
GP2-S	1 A g^{-1}	302	[S30]
PANI/GMS	0.5 A g^{-1}	261	[S31]
G-PNF_{30} film	0.3 A g^{-1}	210	[S32]
PANI-GNRs-40	0.25 A g^{-1}	340	[S33]
PANi/graphene hydrogel	0.4 A g^{-1}	223.8	[S34]
graphene platelet/PANI film	20 mV s^{-1}	269	[S35]
TAG_{Ni}	**0.5 A g^{-1}**	**335.2**	**This work**
TAG_{Cu}	**0.5 A g^{-1}**	**382.5**	**This work**
TAG_{Fe}	**0.5 A g^{-1}**	**351.9**	**This work**

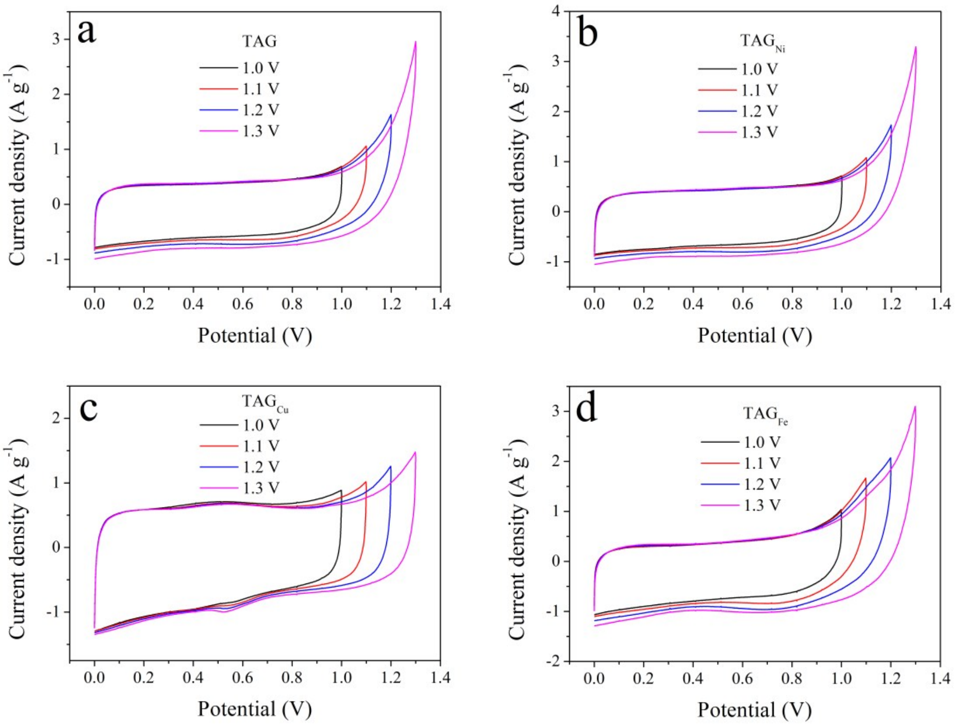

Fig. S12 The CV curves of TAG, TAG_{Ni}, TAG_{Cu} and TAG_{Fe} under different potential range at 10 mV s^{-1}.

Table S7 Comparison of energy density of TAG_{Ni}, TAG_{Cu} and TAG_{Fe} with reported conducting polymer, conducting polymer/carbon composites and biomass based composites.

Materials	E ($Wh\ kg^{-1}$)	P ($W\ kg^{-1}$)	Reference
graphene/PANI@cc	11.38	199.8	[S36]
PPy/RGO-10	7.02	89	[S29]
GP2-S	10.2	250	[S30]
BC/GE/PANI	14.2	200	[S37]
PANI-GNRs-40	7.56	3149	[S33]
graphene/PANI films	18.7	125	[S32]
PPH-5	18.7	125	[S38]
PANI/graphene hydrogel	12.1	40	[S39]
PANI/CNT film	7.1	2189	[S40]
graphene platelet/PANI film	9.3	454	[S35]
3D-G/PANI film	15.1	400	[S41]
CNF/RGO/CNT	8.1	2700	[S10]
TAG_{Ni}	**16.76**	**300**	**This work**
TAG_{Cu}	**19.13**	**300**	**This work**
TAG_{Fe}	**17.6**	**300**	**This work**

References:

[S1] Y. Shi, L. Pan, B. Liu, Y. Wang, Y. Cui, Z. Bao and G. Yu. *J. Mater. Chem. A*, **2014**, *2*, 6086-6091.

[S2] K. Wang, X. Zhang, C. Li, H. Zhang, X. Sun, N. Xu and Y. Ma. *J. Mater. Chem. A*, **2014**, *2*, 19726-19732.

[S3] F. Yang, M. Xu, S.-J. Bao, H. Wei and H. Chai. *Electrochim. Acta*, **2014**, *137*, 381-387.

[S4] Z. Niu, L. Liu, L. Zhang, Q. Shao, W. Zhou, X. Chen and S. Xie. *Adv. Mater.*, **2014**, *26*, 3681-3687.

[S5] Z. Tai, X. Yan and Q. Xue. *J. Electrochem. Soc.*, **2012**, *159*, A1702-A1709.

[S6] Y. Zhao, J. Liu, Y. Hu, H. Cheng, C. Hu, C. Jiang, L. Jiang, A. Cao and L. Qu. *Adv. Mater.*, **2013**, *25*, 591-595.

[S7] R. Sun, H. Chen, Q. Li, Q. Song and X. Zhang. *Nanoscale*, **2014**, *6*, 12912-12920.

[S8] T. Ni, L. Xu, Y. Sun, W. Yao, T. Dai and Y. Lu. *ACS Sustainable Chem. Eng.*, **2015**, *3*, 862-870.

[S9] K. Gao, Z. Shao, J. Li, X. Wang, X. Peng, W. Wang and F. Wang. *J. Mater. Chem. A*, **2013**, *1*, 63-67.

[S10] Q. Zheng, Z. Cai, Z. Ma and S. Gong. *ACS Appl. Mater. Interfaces*, **2015**, *7*, 3263-3271.

[S11] H. Xu, H. Jiang, X. Li and G. Wang. *RSC Adv.*, **2015**, *5*, 76116-76121.

[S12] S. K. Kim, Y. K. Kim, H. Lee, S. B. Lee and H. S. Park. *ChemSusChem*, **2014**, *7*, 1094-1101.

[S13] L. Zhu, L. Wu, Y. Sun, M. Li, J. Xu, Z. Bai, G. Liang, L. Liu, D. Fang and W. Xu. *RSC Adv.*, **2014**, *4*, 6261-6266.

[S14] Y. Song, J. Yang, K. Wang, S. Haller, Y. Wang, C. Wang and Y. Xia. *Carbon*, **2016**, *96*, 955-964.

[S15] Y. Chen, Z. Gao, B. Zhang, S. Zhao and Y. Qin. *J. Power Sources*, **2016**, *315*, 254-260.

[S16] M. Enterría, F. J. Martín-Jimeno, F. Suárez-García, J. I. Paredes, M. F. R. Pereira, J. I. Martins, A. Martínez-Alonso, J. M. D. Tascón and J. L. Figueiredo. *Carbon*, **2016**, *105*, 474-483.

[S17] J. Wang, B. Li, T. Ni, T. Dai and Y. Lu. *Compos. Sci. Technol.*, **2015**, *109*, 12-17.

[S18] F. Zhang, F. Xiao, Z. H. Dong and W. Shi. *Electrochim. Acta*, **2013**, *114*, 125-132.

[S19] H. Zhou, T. Ni, X. Qing, X. Yue, G. Li and Y. Lu. *RSC Adv.*, **2014**, *4*, 4134-4139.

[S20] W. Ouyang, J. Sun, J. Memon, C. Wang, J. Geng and Y. Huang. *Carbon*, **2013**, *62*, 501-509.

[S21] C. Yang and D. Li. *Mater. Lett.*, **2015**, *155*, 78-81.

[S22] S. Admassie, A. Elfwing, E. W. H. Jager, Q. Bao and O. Inganäs. *J. Mater. Chem. A*, **2014**, *2*, 1974-1979.

[S23] F. N. Ajjan, N. Casado, T. Rębiś, A. Elfwing, N. Solin, D. Mecerreyes and O.

Inganäs. *J. Mater. Chem. A*, **2016**, *4*, 1838-1847.

[S24] Q. Xie, S. Zhou, A. Zheng, C. Xie, C. Yin, S. Wu, Y. Zhang and P. Zhao. *Electrochim. Acta*, **2016**, *189*, 22-31.

[S25] X. Li, J. Zhou, W. Xing, F. Subhan, Y. Zhang, P. Bai, B. Xu, S. Zhuo, Q. Xue and Z. Yan. *Electrochim. Acta*, **2016**, *190*, 923-931.

[S26] J. Yin, Y. Zhu, X. Yue, L. Wang, H. Zhu and C. Wang. *Electrochim. Acta*, **2016**, *201*, 96-105.

[S27] Y. A. Lee, J. Lee, D. W. Kim, C.-Y. Yoo, S. H. Park, J. J. Yoo, S. Kim, B. Kim, W. K. Cho and H. Yoon. *J. Mater. Chem. A*, **2017**, *5*, 25368-25377.

[S28] Y. Han, T. Wang, T. Li, X. Gao, W. Li, Z. Zhang, Y. Wang and X. Zhang. *Carbon*, **2017**, *119*, 111-118.

[S29] J. Zhu, Y. Xu, J. Wang, J. Wang, Y. Bai and X. Du. *Phys. Chem. Chem. Phys.*, **2015**, *17*, 19885-19894.

[S30] T. Huang, S. Cai, H. Chen, Y. Jiang, S. Wang and C. Gao. *J. Mater. Chem. A*, **2017**, *5*, 8255-8260.

[S31] H. Cao, X. Zhou, Y. Zhang, L. Chen and Z. Liu. *J. Power Sources*, **2013**, *243*, 715-720.

[S32] Q. Wu, Y. Xu, Z. Yao, A. Liu and G. Shi. *ACS Nano*, **2010**, *4*, 1963-1970.

[S33] L. Li, A. R. Raji, H. Fei, Y. Yang, E. L. Samuel and J. M. Tour. *ACS Appl. Mater. Interfaces*, **2013**, *5*, 6622-6627.

[S34] M. Moussa, Z. Zhao, M. F. El-Kady, H. Liu, A. Michelmore, N. Kawashima, P. Majewski and J. Ma. *J. Mater. Chem. A*, **2015**, *3*, 15668-15674.

[S35] Y. Xu, M. G. Schwab, A. J. Strudwick, I. Hennig, X. Feng, Z. Wu and K. Müllen. *Adv. Energy Mater.*, **2013**, *3*, 1035-1040.

[S36] L. Wen, K. Li, J. Liu, Y. Huang, F. Bu, B. Zhao and Y. Xu. *RSC Adv.*, **2017**, *7*, 7688-7693.

[S37] H. Luo, J. Dong, Y. Zhang, G. Li, R. Guo, G. Zuo, M. Ye, Z. Wang, Z. Yang and Y. Wan. *Chem. Eng. J.*, **2018**, *334*, 1148-1158.

[S38] W. Li, H. Lu, N. Zhang and M. Ma. *ACS Appl. Mater. Interfaces*, **2017**, *9*, 20142-20149.

[S39] Y. Xu, Y. Tao, X. Zheng, H. Ma, J. Luo, F. Kang and Q. H. Yang. *Adv. Mater.*, **2015**, *27*, 8082-8087.

[S40] C. Meng, C. Liu, L. Chen, C. Hu and S. Fan. *Nano Lett.*, **2010**, *10*, 4025-4031.

[S41] K. Li, J. Liu, Y. Huang, F. Bu and Y. Xu. *J. Mater. Chem. A*, **2017**, *5*, 5466-5474.